



CrossMark
click for updates

Research

Cite this article: Padilla-Gamiño JL, Kelly MW, Evans TG, Hofmann GE. 2013 Temperature and CO₂ additively regulate physiology, morphology and genomic responses of larval sea urchins, *Strongylocentrotus purpuratus*. *Proc R Soc B* 280: 20130155.
<http://dx.doi.org/10.1098/rspb.2013.0155>

Received: 22 January 2013

Accepted: 6 March 2013

Subject Areas:

physiology, ecology

Keywords:

global change, multistress, ocean acidification, purple urchin, temperature

Author for correspondence:

Jacqueline L. Padilla-Gamiño

e-mail: gamino@lifesci.ucsb.edu

[†]These authors contributed equally to this study.

Electronic supplementary material is available at <http://dx.doi.org/10.1098/rspb.2013.0155> or via <http://rspb.royalsocietypublishing.org>.

Temperature and CO₂ additively regulate physiology, morphology and genomic responses of larval sea urchins, *Strongylocentrotus purpuratus*

Jacqueline L. Padilla-Gamiño^{1,†}, Morgan W. Kelly^{1,†}, Tyler G. Evans^{1,2} and Gretchen E. Hofmann¹

¹Department of Ecology, Evolution and Marine Biology, University of California Santa Barbara, Santa Barbara, CA 93106, USA

²Department of Biological Sciences, California State University East Bay, Hayward, CA 94542, USA

Ocean warming and ocean acidification, both consequences of anthropogenic production of CO₂, will combine to influence the physiological performance of many species in the marine environment. In this study, we used an integrative approach to forecast the impact of future ocean conditions on larval purple sea urchins (*Strongylocentrotus purpuratus*) from the northeast Pacific Ocean. In laboratory experiments that simulated ocean warming and ocean acidification, we examined larval development, skeletal growth, metabolism and patterns of gene expression using an orthogonal comparison of two temperature (13°C and 18°C) and pCO₂ (400 and 1100 µatm) conditions. Simultaneous exposure to increased temperature and pCO₂ significantly reduced larval metabolism and triggered a widespread downregulation of histone encoding genes. pCO₂ but not temperature impaired skeletal growth and reduced the expression of a major spicule matrix protein, suggesting that skeletal growth will not be further inhibited by ocean warming. Importantly, shifts in skeletal growth were not associated with developmental delay. Collectively, our results indicate that global change variables will have additive effects that exceed thresholds for optimized physiological performance in this keystone marine species.

1. Introduction

Two pervasive consequences of increasing anthropogenic CO₂ are ocean warming and ocean acidification, both of which manifest at a global scale and have important consequences for the structure and function of marine ecosystems [1–3]. To better predict how global change will affect marine communities, it is critical that we understand the interactive effects of multiple global change variables on physiological function [4–6]. However, the combined influence of multiple ocean change factors on performance is complex and poorly understood [6,7]. For example, physiological responses could be primarily driven by a single factor or by multiple factors interacting in an additive, synergistic or antagonistic manner [7,8]. Additionally, multiple stressors may differentially affect specific life cycle stages, with important implications for development, dispersal, physiological tolerance and biogeography [3,4,7,9].

In this study, we used an integrative approach to understand how the larval stage of a keystone species, the purple sea urchin *Strongylocentrotus purpuratus* [10], responds to simulated future ocean warming and ocean acidification. *Strongylocentrotus purpuratus* has a broad biogeographic distribution [11] and is an ecologically and economically important species within the California Current Large Marine Ecosystem (CCLME) [10]. The CCLME is one of the most valuable and productive ecosystems in the world [12] and is already affected by global change [13–15]. Temperature regimes in the CCLME reflect average warming trends in the global ocean and even warming that has occurred in the twentieth century has significantly influenced the structure of marine communities in this region

[13]. Furthermore, the CCLME already experiences considerable declines in pH as a result of upwelling, and ocean acidification is expected to progress rapidly [14,15], with rates of change similar to those projected for the Southern Ocean and Arctic.

Larvae of many important marine organisms within the CCLME already develop in the water column under fluctuating temperature and pCO₂ regimes; however, it is not known whether many species will be able to tolerate future conditions, as the cumulative effects of continued warming and acidification drive organisms closer to the limits of their physiological tolerances [4,5,8,16]. For example, exposure to acidified sea water may act to lower the ceiling of organismal tolerance of high temperatures through changes in metabolism [4,17,18], whereas warmer temperatures may alter the permeability of cell membranes [19] and reduce the ability of organisms to regulate intracellular pH [20]. To explore the potential response of larval purple sea urchins to these co-occurring factors, we cultured larvae under conditions that mimicked future ocean change in the CCLME and assessed organismal performance across multiple levels of biological organization. By exposing early life-stages to different combinations of temperature (13°C and 18°C) and pCO₂ (400 µatm or 1100 µatm), we sought to address the following questions: (i) Do temperature and pCO₂ interact to influence larval skeletal growth and development? (ii) Are there metabolic costs to tolerating high temperature/low pH conditions? and (iii) What are the cellular/molecular mechanisms that underlie physiological responses to coincident global change variables? As the first study to integrate morphological, physiological, developmental and transcriptomic data, our work provides unique insights into the effects of multiple global change stressors on marine organisms.

2. Material and methods

(a) Animal collection and fertilization protocol

Adult *S. purpuratus* were collected by SCUBA at a depth of 5 m near Goleta Pier in the Santa Barbara Channel, California, USA (34° 24.842 N, 119° 59.058 W) in December 2011 and maintained in a flowing sea water system at the University of California Santa Barbara at approximately 15°C. Spawning was induced by intracoelomic injection of 0.5 M KCl, and eggs were collected in 0.35 µm filtered, UV-sterilized sea water (FSW) at approximately 14 °C and 400 µatm pCO₂. Sperm was collected dry and kept on ice until fertilization. Single dam-sire crosses were used (the sperm from one male was used to fertilize the eggs of a single female) in order to include multiple parental lineages and make population-level generalizations more reliable. Fertilizations were performed using water from the low pCO₂ treatment (400 µatm) in order to eliminate confounding effects of high pCO₂ on sperm mobility [21]. After fertilization, embryos for each family were distributed among culture vessels for each pCO₂/temperature treatment at a concentration of approximately 10 embryos ml⁻¹. Although we included multiple parental lineages in the study, for statistical purposes we were not able to distinguish between family and culture vessel effects since we did not have replication for each family and pCO₂/temperature treatment combination.

(b) Larval experimental culture conditions and sea water chemistry

Embryos were cultured using a flow-through CO₂ mixing system as described in Fanguie *et al.* [22]. The system was modified by pumping the appropriate CO₂-gas mix for the treatment into

the headspace of the culture vessels [23]. pCO₂ exposure levels (400 and 1100 µatm) were based upon current conditions and predictions for the CCLME, where anthropogenic inputs of CO₂ are expected to drive surface pH down to 7.6 during upwelling in only a few decades [14]. Temperature was manipulated by holding culture vessels in sea water tables at 13°C or 18°C (±0.6) using a Delta Star heat pump (AquaLogic) and a digital temperature controller (Nema 4x, AquaLogic). Temperature levels were chosen based on present-day thermal profiles (13°C, January–April, Santa Barbara, CA, USA) and IPCC projections for sea surface temperature in southern California during spawning season (18°C, [24]). Temperature, salinity and pH were measured daily for each culture according to best practice procedures outlined by Dickson *et al.* [25] and described in detail by Fanguie *et al.* [22]. Temperature was measured using a wire-thermocouple (Themolyne PM 207000/Series 1218), and salinity was measured using a conductivity meter (YSI 3100). pH was determined following the standard operating procedure (SOP) 6b [25] using a spectrophotometer (Bio Spec-1601, Shimadzu) and dye m-cresol purple (Sigma-Aldrich) as the indicator. Total alkalinity (TA) was measured every day in two of the reservoir buckets, except for the first experimental run in which TA was only measured at the end of the experiment. TA was estimated using the SOP 3b [25]. Both pH and alkalinity were assessed for accuracy using certified reference materials (CRMs) from Dickson (Scripps Institution of Oceanography). Tris buffer in synthetic sea water Batch 8 (pH = 8.0923 ± 0.0004) and Batch 103 (TA = 2232.94 ± 0.79 µmol kg⁻¹) were used as CRM for pH and alkalinity, respectively. pCO₂, Ω_{ara} and Ω_{cal} were estimated using CO₂calc [26] with the carbonic acid dissociation constants of Mehrbach *et al.* [27]. Temperature, salinity and carbonate parameters of sea water used in experimental treatments are shown in the electronic supplementary material, table S1.

(c) Larval collection

Temperature has a direct effect on developmental rate, with marine invertebrate embryos developing faster at high temperatures [28]. As a result, in our experiments, larvae cultured under 18°C are at different developmental stages than those cultured at 13°C, despite being the same age. As it is only possible to control for one of these variables, we chose to exclusively compare larvae at the same developmental stage rather than age (for details, see the electronic supplementary material, figure S1).

(d) Developmental progression

Development was tracked by recording the proportion of embryos to reach gastrula and early pluteus stages under each experimental condition (*n* = 4, for each experimental condition). Cultures were monitored by removing 50 larvae every 2 h and scoring each larva as complete or incomplete for having reached either gastrula or early pluteus. The experiment was terminated when all 50 of the sampled larvae were scored as complete. We considered embryos as gastrulae when the tip of the archenteron made contact with the overlying ectoderm near the animal pole and early plutei when the surface between the dorsal arms became concave and the apical tip of the larva became pointed (figure 1). Differences in development were tested using a logistic regression where stage (complete versus incomplete) was the dependent variable, pCO₂ level (high versus low) and temperature (high versus low) were treated as fixed effects and time since fertilization was treated as a random effect. Statistical tests were performed in R [29].

(e) Body size

Pluteus stage larvae were collected at 94 h and 116 h after fertilization, for high and low temperatures, respectively (*n* = 8, for

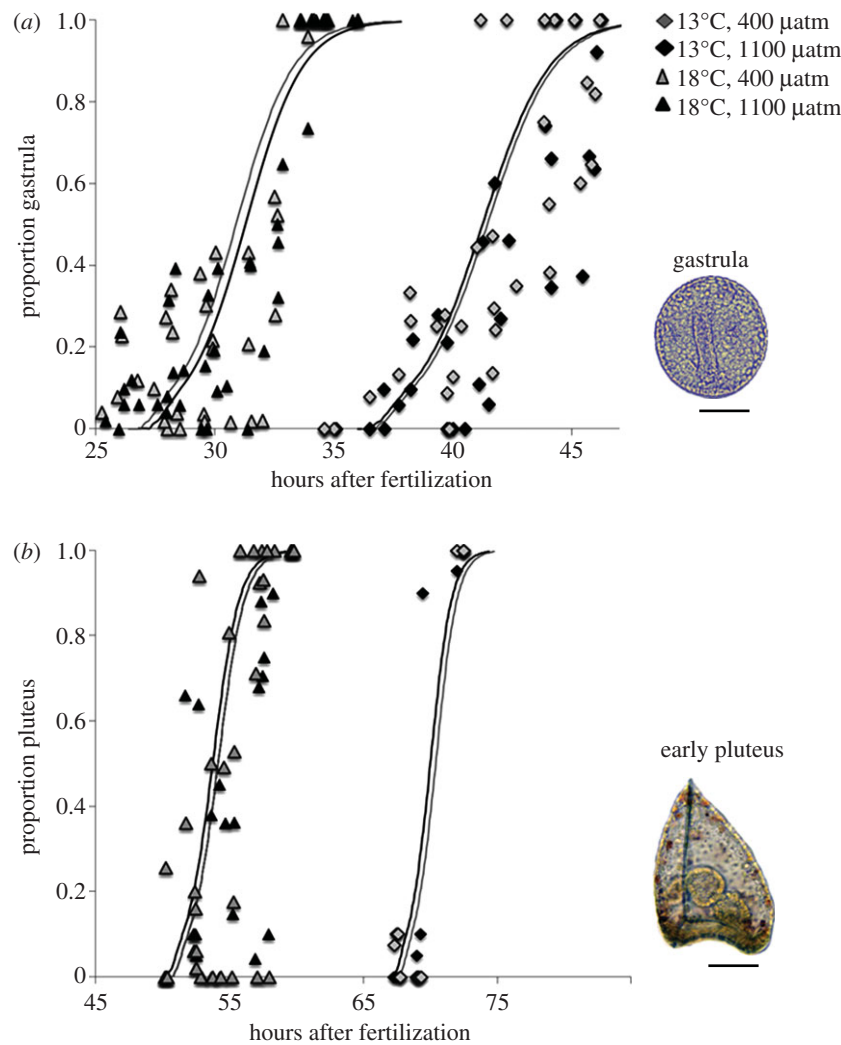


Figure 1. Developmental progression in *Strongylocentrotus purpuratus* at different temperature and pCO₂ treatments during gastrulation (a) and early pluteus development (b). Developmental progression changes under different temperatures but not under different pCO₂ treatments. Scale bar, 75 μm.

each experimental condition), and immediately fixed in 2 per cent formalin saturated with sodium borate to prevent acidity and dissolution of the skeleton. Photographs for morphometric analyses were taken within two weeks of fixation, under 10× compound magnification (Olympus, BX50, Lumenera, Infinity Lite) with larvae orientated dorsal side down. Overall skeletal length ($n = 20$ /culture vessel) was estimated by measuring the distance from the spicule tip of the left postoral arm to the spicule tip of the aboral end. Additional body size measurements (arm length, body length at midline and stomach) were performed in a subset of samples to confirm the patterns observed in the overall skeletal length measurements (see the electronic supplementary material, figure S2). Differences in body size measurements between treatments were tested using a two-way ANOVA with temperature and pCO₂ as fixed factors.

(f) Respirometry

Rates of oxygen consumption were obtained in early pluteus larvae ($n = 6$, 70 h and 92 h after fertilization for high and low temperatures, respectively) according to [30] with modifications. In brief, different densities of larvae (50–600 individuals) were placed in each respiratory chamber (684–795 μl vials) and incubated for 4–7 h in order to generate a standard curve from which we could estimate the rate of oxygen consumption per individual (expressed as pmol O₂/hr/larva) under each experimental condition. Two control vials containing only FSW were incubated simultaneously to account for background respiration. Following

incubation, larvae were removed, water was transferred to an optode cell using a gastight syringe (Hamilton Company, USA) and O₂ measured using a fibre-optic oxygen meter (PreSens, Microx TX3, Germany). The oxygen metre was calibrated using NaSO₃ solution and FSW (0.01 g per ml). Additional blanks (FSW only) were used to account for systematic time variation of the instrumental zero value (instrumental drift). Differences in respiratory rates among treatments were tested using a two-way ANOVA, with temperature and pCO₂ as fixed factors. Q_{10} values for each pCO₂ treatment were estimated using the van't Hoff equation [31]. Linear regression was used to determine the relationship between larval size and respiration. The regression was performed using the average respiration rate and average body size for each family.

(g) Changes in the transcriptome

(i) RNA extraction, amplification and labelling

A total of 12 samples were used for transcriptional profiling, corresponding to larvae collected from three replicate cultures across each experimental condition. Pluteus stage samples, containing approximately 9000 larvae, were acquired from the same families as used in respiration and morphometrics. Larvae were concentrated into a small volume of sea water using reverse filtration, transferred to 1.5 ml Eppendorf tubes and quickly pelleted by centrifugation. Reverse filtration was performed by drawing sea water through a fine mesh screen (35 μm), such that the volume of sea water was gradually reduced but the embryos

remained in the solution, a process taking approximately 5 min. After centrifugation, excess water was then removed, larvae were flash frozen in liquid nitrogen and 1 ml of TRIzol Reagent (Invitrogen, Carlsbad, CA, USA) was added. Total RNA was extracted using the guanidine isothiocyanate method [32]. Following extraction, RNA was processed to remove tRNA and degraded fragments using a RNeasy Mini Kit according to manufacturer's instructions (Cat. no. 74104, Qiagen, Valencia, CA, USA). RNA yield and purity were assessed by measuring A260 and A260/A280 ratio, respectively, with a NanoDrop spectrophotometer (NanoDrop Technologies, Wilmington, DE, USA). Two hundred nanograms of clean, total RNA from either experimental or reference samples were amplified and labelled with Cy5 or Cy3, respectively, using Agilent's Low Input Quick Amp Two-Color Labeling Kit (no. 5190-2306, Agilent Technologies Inc., Santa Clara, CA, USA). Each amplification and labelling reaction also contained 'spike-in' RNA (Agilent's Two-Color RNA Spike-In Kit, no. 5188 5279, Agilent Technologies Inc.), which generate expected fluorescent signal intensities used in quality control. Yield and specific activity of the resulting amplified and labelled RNA was determined using a NanoDrop spectrophotometer (NanoDrop Technologies). In accordance with suggested standards (Agilent Technologies Inc.), only amplified and labelled RNA whose yield and specific activity exceeded 1.875 µg and 6 pmol of fluorescent dye incorporation per microgram RNA, respectively, were used in subsequent hybridizations.

(ii) Gene expression profiling with microarrays

Transcriptional profiling was performed using custom-designed 105 000 feature oligonucleotide microarrays (Agilent Technologies Inc.) with coverage of all 28 036 putative genes in the *S. purpuratus* genome as described in [33]. Gene expression levels were determined by comparing the amount of RNA transcript in experimental samples relative to a common reference sample, whereby experimental samples were fluorescently tagged with Cy5 (red) dye and the reference with Cy3 (green) dye. Resulting fluorescent images were captured with an Axon GenePix 4000B microarray scanner (Axon Instruments, Sunnyvale, CA, USA). Only features whose locally weighted scatterplot smoothing (LOWESS) normalized signal intensities were 2.6 times background level but below the saturation threshold on all 12 arrays were included in further analyses. Expression was summarized across multiple probes targeting the same putative gene loci by computing the geometric mean. Resulting signal intensities were then converted to log₂-ratios of the experimental channel (Cy5) divided by the reference channel (Cy3). Log₂-ratio expression data for this set of 3627 genes was then used in downstream statistical analyses. Microarray data were submitted to the Gene Expression Omnibus (<http://www.ncbi.nlm.nih.gov/geo/>; GSE39125 and GPL15481).

Microarray expression data were analysed using principal component analysis (PCA), singular value decomposition (SVD; [34]) and gene set enrichment analysis (GSEA). PCA identifies axes of maximal variance and was used to illustrate the relative contribution of experimental conditions (i.e. temperature and pCO₂) to the variation in gene expression. We evaluated the results of the PCA using loading plots, whereby the spatial clustering of experimental samples on the plot reflects the degree of similarity between transcriptomes. For the PCA, we used the normalized log₂-ratio data of all genes passing filtering criteria, averaging their expression across each of the three replicates at each treatment. PCA was computed using the correlation matrix and was conducted in the R statistical programming environment [29]. SVD was used to identify genes responsible for the largest proportion of variation in the gene expression dataset. SVD is a data-reduction technique in which the expression dataset is reduced to a series of 'eigen genes,' each corresponding to a major expression pattern [35]. Pearson correlation coefficients

were calculated for genes whose mean expression changed >1.5-fold between treatment groups to identify genes whose expression defines the dominant patterns detected by SVD (greater than 0.8). Finally, we used GSEA to resolve the biological significance of genes responding to pCO₂ and/or temperature [36]. GSEA is a statistical tool that uses functional information to identify categories of genes (i.e. ontologies) significantly over- or under-represented within a user-defined list. Significance is determined by the binomial statistic, and we considered ontologies with Benjamini and Hochberg corrected *p*-values less than 0.05 to be significant.

3. Results

To gain insight into the effects of future ocean change on *S. purpuratus* at different levels of biological organization, we designed laboratory experiments that mimicked present temperature and pCO₂ conditions (13°C, 400 µatm) and future scenarios owing to increased anthropogenic CO₂ (18°C, 1100 µatm). Following culturing, we measured four response variables in urchin early life-stages: developmental progression, body size (with size of the calcium carbonate skeleton serving as proxy), respiration rate and alterations in the transcriptome.

(a) Developmental progression

Early development from embryo through pluteus stage progressed normally, and no obvious morphological abnormalities were observed under any of the experimental conditions. As expected, the pace of development increased as a function of temperature ($Z = 24.5$, d.f. = 1, $p < 0.001$, $Z = 34.1$, d.f. = 1, $p < 0.001$, gastrula and pluteus, respectively, figure 1*a,b*). However, pCO₂ did not affect the rate of development at either temperature and embryos reached obvious developmental landmarks synchronously ($Z = 0.7$, d.f. = 1, $p = 0.3$, $Z = 6.7$, d.f. = 1, $p = 0.3$, gastrula and pluteus, respectively, figure 1*a,b*).

(b) Body size

pCO₂ had a significant effect on overall skeletal length (figure 2*a*, $F = 34.38$, d.f. = 1, $p < 0.001$). Skeletons of pluteus stage larvae were approximately 8 per cent smaller in high pCO₂ treatments relative to low pCO₂ treatments at both temperatures. Arm length and body length at midline measurements also showed a significant decrease under high pCO₂ ($F = 10.27$, d.f. = 1, $p = 0.006$; $F = 10.78$, d.f. = 1, $p = 0.005$, respectively, electronic supplementary material, figure S2). pCO₂ did not have a significant effect on stomach area ($F = 1.4$, d.f. = 1, $p = 0.255$). Temperature did not have an effect on overall skeletal length (figure 2*a*, $F = 0.01$, d.f. = 1, $p = 0.908$), arm length ($F = 0.28$, d.f. = 1, $p = 0.604$), body length at midline ($F = 0.41$, d.f. = 1, $p = 0.533$) or stomach area ($F = 0.10$, d.f. = 1, $p = 0.762$) after controlling for developmental stage.

(c) Respiration rate

Both temperature and pCO₂ had a significant effect on larval respiration (figure 2*b*, $F = 19.06$, d.f. = 1, $p < 0.001$; $F = 5.23$, d.f. = 1, $p = 0.033$, respectively). At 18°C, respiration rates significantly decreased (23%) in the high pCO₂ treatment ($p = 0.0385$, figure 2*b*). By contrast, respiration rates did not significantly change between high and low pCO₂ treatments

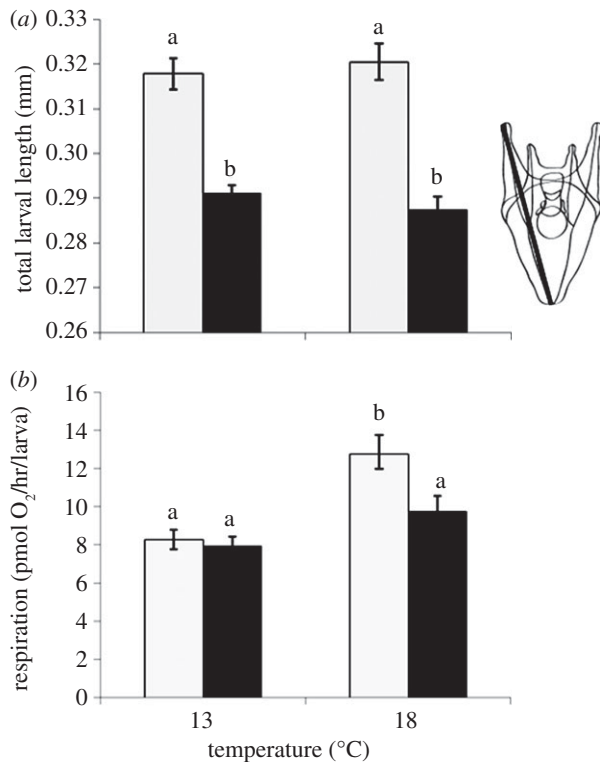


Figure 2. Physiological performance of *S. purpuratus* under different temperature and pCO₂ treatments. (a) Morphometrics and (b) respiration rates. Data are mean \pm s.e. with different letters indicating statistical significance ($p < 0.05$). Skeletal growth differed between pCO₂ treatments but did not differ between temperatures. Respiratory rates between pCO₂ treatments did not differ at 13°C but differed at 18°C. Filled bars, 1100 μ atm; unfilled bars, 400 μ atm.

at 13°C ($p = 0.9895$, figure 2b). Larvae exposed to 400 μ atm had higher (35%) respiration rates at 18°C than at 13°C ($p = 0.0015$), whereas larvae exposed to 1100 μ atm did not have significantly different respiratory rates between temperature treatments ($p = 0.3122$), indicating that elevated pCO₂ seems to have counteracted the expected effect of increased temperature on metabolic rate. The decrease in larval metabolic rate at 18°C/high pCO₂ was reflected in a lower Q₁₀, reduced under high pCO₂ from 2.49 to 1.55. There was no significant interaction between temperature and pCO₂ ($F = 3.42$, d.f. = 1, $p = 0.079$) and no correlation between respiration rate and larval body size ($p = 0.705$).

(d) Changes in the transcriptome

Genome wide transcriptomics were used to provide mechanistic insight into pathways or processes that might be linked to the observations made on two organismal traits—differences in total larval length and respiration rate between experimental conditions. As an initial broad-scale analysis, we used a principal components loading plot to resolve the relationship between temperature, pCO₂ and gene expression. This plot revealed that the transcriptomes of larvae raised at 13°C were most similar, as the high and low pCO₂ treatments at 13°C clustered most closely. Transcriptional profiles diverged in larvae raised at 18°C as well as between high and low pCO₂ treatments (see the electronic supplementary material, figure S3). These expression patterns were corroborated by SVD, which revealed two major patterns of gene expression that collectively accounted for 89 per cent of the total

variation in gene expression. The first expression pattern (i.e. eigengene 1, figure 3a) accounted for 64 per cent of the variation and is described by genes whose expression increased in response to elevated temperature and decreased in response to high pCO₂ (figure 3a). One-hundred and eleven genes were positively correlated (greater than 0.8) with this expression pattern (see figure 3b and electronic supplementary material, table S2a). We used GSEA to identify physiological and cellular processes influenced by the differential expression of these genes. Ontologies relating to the cellular cytoskeleton were by far the most numerous and had the lowest p -values, accounting for 22 of the 42 enriched ontologies (52%) and ontologies with the 11 lowest p -values. Genes driving the enrichment of these cytoskeletal ontologies included multiple isoforms of alpha tubulin and beta tubulin, as well as actin. Other cytoskeletal genes differentially expressed included kinesin-like protein KIF3A (P28741), apextrin (A0T3F5), syntenin (O00560) and ankyrin domain repeat containing protein 28 (Q9UPS8) (uniprot identifiers in parenthesis; www.uniprot.org). We also surveyed these same 111 genes correlated with eigengene 1 for genes with established roles in larval skeletogenesis and whose altered expression may be associated with the observed changes in skeletal morphology. Spicule matrix 30 alpha protein (SM30-alpha protein), a major component of urchin larval skeletons [37], was downregulated in larvae raised in high pCO₂ water at both temperatures.

The pattern responsible for the second largest proportion of variation in expression (i.e. eigengene 2; 25%; figure 3c) described genes decreasing between low and high pCO₂ treatments at 18°C. Forty-nine genes were positively correlated (greater than 0.8) with this expression pattern (see figure 3d and electronic supplementary material, table S2a). As previously explained, we used GSEA to identify larger-scale physiological and cellular processes influenced by the differential expression of these genes. Ontologies relating to nucleosome and chromatin organization and assembly accounted for 14 of 21 significantly over-represented ontologies (67%) and 27 of 49 differentially expressed genes encode histones, structural components of nucleosomes and major regulators of chromatin structure and transcription initiation, processes that are central to the regulation of the cell cycle. Included were histone 2AE, 2AD, 2BF, 2BC, H2B, H3F, H3D, CS-H3, H3 and H3 family 2 isoform 2. Complete GSEA results are shown in the electronic supplementary material, table S2b. Genes encoding skeletal matrix proteins were not present in the set of genes correlated with eigengene 2.

4. Discussion

The central goal of this study was to capture the cumulative effects of multiple global change-related stressors on the physiology of calcifying marine larvae. Our integrative approach yielded important findings relevant to the performance of *S. purpuratus* in future oceans. Firstly, skeletal growth but not developmental rate was influenced by elevated pCO₂. Secondly, simultaneous exposure to both increased pCO₂ and temperature significantly depressed larval metabolism. Thirdly, transcriptional responses suggest that (i) decreases in skeletal length at high pCO₂ may be associated with impaired skeletogenesis, (ii) metabolic depression in response to elevated temperature and pCO₂ were associated with reduced expression of multiple histone encoding genes

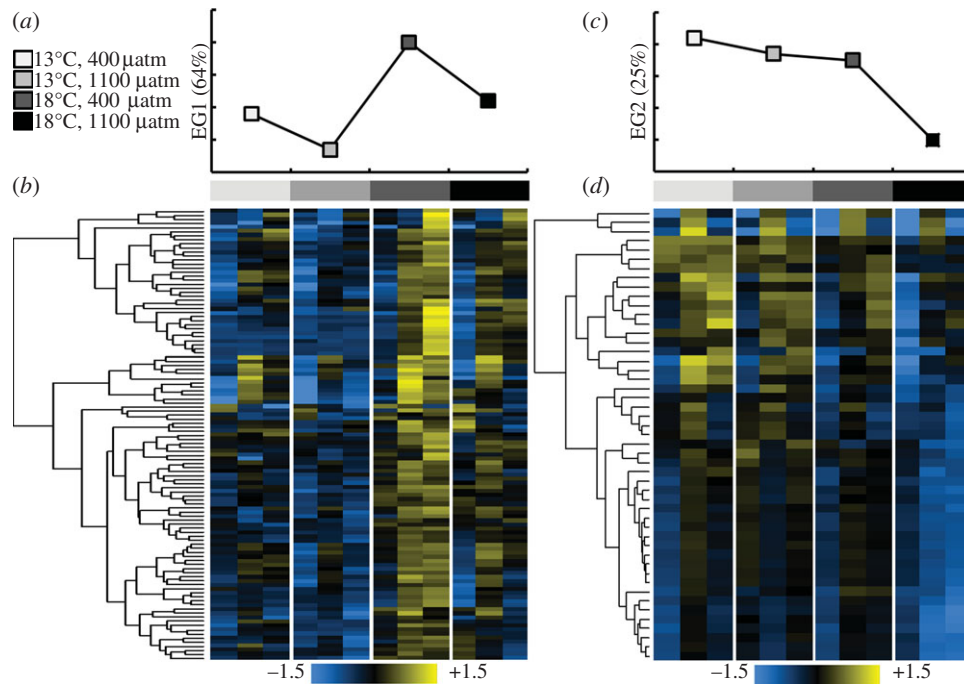


Figure 3. Temperature and/or $p\text{CO}_2$ induced changes gene expression. (a) eigengene 1 (EG1). (b) Hierarchical clustered heatmap of genes positively correlated (greater than 0.8) with EG1. (c) eigengene 2 (EG2). (d) Hierarchical clustered heatmap of genes positively correlated (greater than 0.8) with EG2. Heatmaps display the normalized \log_2 -ratio for each gene (rows) across each replicate at the four temperature and $p\text{CO}_2$ exposures (columns). Ordered gene lists are provided in the electronic supplementary material, table S2a.

potentially reflecting chromatin remodelling owing to changes in the metabolic state of the cell and (iii) basic components of the cellular cytoskeleton, such as actin and tubulin, increased expression in response to elevated temperature, but decreased expression at high $p\text{CO}_2$.

Exposure to elevated $p\text{CO}_2$ has been consistently shown to reduce skeletal growth in larval echinoderms [23,38–42], a finding that we corroborate here. Importantly, our data indicate that this effect was not exacerbated by increases in temperature. Nonetheless, ocean acidification-driven reductions in skeletogenesis are likely to have important ecological and functional implications. Ecologically, if reduced skeletogenesis translates into an overall decrease in larval size, energy transfer across trophic levels may be perturbed as smaller larvae will support fewer or smaller marine consumers [43]. In addition smaller larvae have been shown to be more vulnerable to predation, potentially influencing predator–prey dynamics in marine food webs [44]. From a functional perspective, shifts in skeletal morphology caused by acidification may influence feeding in echinoderms [45], as food capture depends upon the surface area of the ciliary bands covering the larval arms [46]. Even very small reductions in band length can significantly reduce feeding rates [47]. For example, in the echinoid *Dendraster excentricus*, maximum clearance rates (volume of water cleared of food per time) increased with ciliated band length regardless of food availability, a 7 per cent reduction in band length resulted in a 16 per cent reduction in clearance rates [47]. Finally, the ability of larvae to disperse could be affected by changes in skeletal morphology owing to differences in swimming performance [48,49].

Previous research has attributed the inhibitory effect of $p\text{CO}_2$ on skeletogenesis to developmental delay [50], metabolic depression [51,52] and/or a decreased capacity for calcification [53]. Our data show that although highly sensitive to temperature, development was not delayed by $p\text{CO}_2$

and larvae from both $p\text{CO}_2$ treatments reached obvious developmental landmarks synchronously. This is consistent with previous studies that did not detect differences in cell cycle progression (first mitotic division, onset of DNA synthesis and mitotic spindle formation) and developmental timing (prism and early pluteus) in *S. purpuratus* [54–56]. Similarly, experiments in the sea urchin *Heliocidaris erythrogramma* and the sea star *Meridiastra calcar*, found that warming, not acidification, had the dominant effect on development [42,57,58]. Interestingly, Stumpp *et al.* [50] detected developmental delay in the larvae of *S. purpuratus* cultured under high $p\text{CO}_2$ conditions. However, this study used morphometric differences in larval skeletons as a measure of developmental delay rather than the staging based on developmental landmarks used here. The connection between morphometric measurements and developmental stage is tenuous, because of the extensive morphological variation that can exist in larvae within the same developmental stage owing to genetic and environmental factors [59–61]. Our data also largely refute the hypothesis that reduced skeletogenesis is a consequence of reduced metabolism. Reduction in skeletal length was similar at high $p\text{CO}_2$ for both 13°C and 18°C despite different patterns of respiration; there was a reduction in respiration rates in the 18°C/high $p\text{CO}_2$ treatment but no comparable reduction in metabolism for the high $p\text{CO}_2$ treatment at 13°C. Instead, our data support the hypothesis that the effects of $p\text{CO}_2$ on skeletal length are caused by a compromised ability to calcify. Transcriptomics showed that spicule matrix 30 alpha protein (SM30-alpha protein) was downregulated at two different loci between low and high $p\text{CO}_2$ treatments at both 13°C and 18°C. Spicule matrix proteins participate exclusively in calcification and SM30 proteins are considered the principal occluded protein of the developing urchin skeleton [37]. Downregulation of SM30-alpha in response to elevated

pCO₂ is a strong indicator that skeletogenesis is impaired in high pCO₂ sea water and provides a mechanistic explanation for reductions in larval size at elevated pCO₂ [62].

Our results indicate that simultaneous exposure to warmer and more acidic environments can trigger metabolic depression in *S. purpuratus*. Metabolic depression is an adaptive strategy that may allow organisms to tolerate acute short-term stress, whereby energetically expensive processes are temporarily suppressed in order to extend the duration of tolerance [4,53]. *Strongylocentrotus purpuratus* larvae may use metabolic depression to ensure appropriate use of limited energy resources since early larvae are largely dependent on a fixed supply of maternally deposited yolk to fuel development. Interestingly, downregulation of histone encoding genes was the principal transcriptional response accompanying metabolic depression and provided important mechanistic insight into the physiological consequences of coincident rises in temperature and pCO₂. Because no differences in developmental rates were found between CO₂ treatments, we hypothesize that histones may be acting as metabolic sensors [63] and involved in chromatin remodelling rather than indicating repressed cell division [64]. Histones are dynamic proteins that can undergo multiple types of post-translational modifications and play an important role in regulating chromatin function and gene expression depending on the metabolic state of the cell and cofactor concentrations [63,65,66]. One plausible explanation is that larvae simultaneously exposed to increased temperature and pCO₂ exhausted maternal energy supplies more rapidly than larvae in other treatments, possibly reducing key metabolites for histone-modifying enzymes and inducing chromatin remodelling [63,67]. Chromatin remodelling complexes (remodellers) can work with other chromatin factors to control DNA packaging and unpackaging and perform diverse functions such as sliding or ejecting of the nucleosome [68]. Importantly, metabolic depression only affords temporary resistance to environmental stress [53,69], thus these data suggest that high CO₂ and temperature conditions may exceed the capacity for acclimatization in *S. purpuratus* larvae. It is interesting to note that cumulative metabolic effects of ocean warming and ocean acidification on *S. purpuratus* larvae were additive and not synergistic, indicating that these stressors do not exacerbate each other's metabolic effects [8].

Our gene expression data also indicate that the cytoskeleton is sensitive to shifts in temperature and pCO₂: genes encoding fundamental components of the cellular cytoskeleton such as actin and alpha and beta tubulins were upregulated under elevated temperature, but downregulated under elevated pCO₂ (eigengene 1; figure 3). In urchin larvae, the cytoskeleton regulates basic aspects of development, such as cell migration, mitosis and cytokinesis, organelle movements, ciliary and flagellar movements and cell shape changes [70],

and the protection of cytoskeletal function is likely to be important for the completion of development. Transcriptomic and proteomic analysis of mussels (*Mytilus* spp.) from the California Current supports this hypothesis and indicates that the protection of the cytoskeleton is not only a key response to acute heat stress but may also underlie the evolution of increased thermotolerance [71,72]. Nonetheless, the induction of cytoskeletal proteins was lower when both temperature and pCO₂ were increased, implying that simultaneous exposure to high temperature and pCO₂ can affect the cytoskeleton differently than when either stressor is applied independently, and given the role played by the cytoskeleton in basic cellular processes, this may have unresolved consequences for cell function in future oceans.

Global change is a multi-dimensional problem that can affect organisms at many levels of biological organization and at multiple life-history stages [3,7,73]. Here, we present data showing that ocean warming and ocean acidification have additive effects on the performance of larval stages of a keystone species in the CCLME, an ecologically and economically important marine ecosystem already affected by global change. Most notably, simultaneous exposure to increased temperature and pCO₂ led to depressed metabolism and triggered transcriptional changes indicative of chromatin remodelling, suggesting that cumulative effects of multiple stressors may exceed tolerance thresholds for key physiological processes. Impaired larval growth, as evidenced by truncated skeletogenesis and decreased expression of a major spicule matrix protein, was driven exclusively by pCO₂-induced acidification and will not be exacerbated by ocean warming. Finally, an ability to protect cytoskeletal functions during development may be limited by coincident increases in temperature and pCO₂. From a broader global change biology perspective, organisms generally have three responses to environmental change: (i) migration (i.e. range shifts), (ii) using existing physiological plasticity to tolerate local conditions (i.e. acclimatization) and (iii) evolutionary adaptation. However, if future oceans do indeed exceed thresholds for optimized physiological performance as our data suggest, *S. purpuratus* may depend upon migration or rapid adaptation to persist in a high temperature, high pCO₂ ocean.

The authors thank the reviewers for their helpful comments and P. C. Yu, L. Kapsenberg, P. G. Matson, E. B. Rivest, E. Fabris, K. Johnson, P. Quiroga and K. Savicki for logistical support and Christoph Pierre for urchin collection. J.L.P.G. and G.E.H. were partially supported by NSF IOS-1021536 and OCE 1040960 (<http://omegas.science.oregonstate.edu/>). M.W.K. and G.E.H. were supported by funds from the University of California in support of a multi-campus research programme, Ocean Acidification: A Training and Research Consortium (<http://oceanacidification.msi.ucsb.edu/>).

References

1. Hoegh-Guldberg O, Bruno JF. 2010 The impact of climate change on the world's marine ecosystems. *Science* **328**, 1523–1528. (doi:10.1126/science.1189930)
2. Kroeker KJ, Micheli F, Gambi MC, Martz TR. 2011 Divergent ecosystem responses within a benthic marine community to ocean acidification. *Proc. Natl Acad. Sci. USA* **108**, 14 515–14 520. (doi:10.1073/pnas.1107789108)
3. Doney SC *et al.* 2012 Climate change impacts on marine ecosystems. *Ann. Rev. Mar. Sci.* **4**, 11–37.
4. Pörtner HO, Farrell AP. 2008 Ecology physiology and climate change. *Science* **322**, 690–692. (doi:10.1126/science.1163156)
5. Somero GN. 2010 The physiology of climate change: how potentials for acclimatization and genetic adaptation will determine 'winners' and 'losers'. *J. Exp. Biol.* **213**, 912–920. (doi:10.1242/jeb.037473)
6. Boyd PW. 2011 Beyond ocean acidification. *Nat. Geosci.* **4**, 273–274. (doi:10.1038/ngeo1150)
7. Byrne M. 2011 Impact of ocean warming and ocean acidification on marine invertebrate life history stages: vulnerabilities and potential for persistence in a changing ocean. *Oceanogr. Mar. Biol. Annu. Rev.* **49**, 1–42.
8. Crain CM, Kroeker K, Halpern BS. 2008 Interactive and cumulative effects of multiple human stressors

- in marine systems. *Ecol. Lett.* **11**, 1304–1315. (doi:10.1111/j.1461-0248.2008.01253.x)
9. O'Connor MI, Bruno JF, Gaines SD, Halpern BS, Lester SE, Kinlan BP, Weiss JM. 2007 Temperature control of larval dispersal and the implications for marine ecology, evolution, and conservation. *Proc. Natl Acad. Sci. USA* **104**, 1266–1271. (doi:10.1073/pnas.0603422104)
 10. Pearse JS. 2006 Perspective: ecological role of purple sea urchins. *Science* **314**, 940–941. (doi:10.1126/science.1131888)
 11. Tegner MJ. 2001 The ecology of *Stroglyocentrotus franciscanus* and *Stroglyocentrotus purpuratus*. In *Edible sea urchins: biology and ecology* (ed. JM Lawrence), pp. 307–331. New York, NY: Elsevier.
 12. Costanza R *et al.* 1997 The value of the world's ecosystem services and natural capital. *Nature* **387**, 253–260. (doi:10.1038/387253a0)
 13. Field DB, Baumgartner TR, Charles CD, Ferreira-Bartrina V, Ohman MD. 2006 Planktonic foraminifera of the California Current reflect 20th-century warming. *Science* **311**, 63–66. (doi:10.1126/science.1116220)
 14. Hauri C, Gruber N, Plattner GK, Alin S, Feely RA, Hales B, Wheeler PA. 2009 Ocean acidification in the California current system. *Oceanography* **22**, 60–71. (doi:10.5670/oceanog.2009.97)
 15. Gruber N, Hauri C, Lachkar Z, Loher D, Frolicher TL, Plattner G. 2012 Rapid progression of ocean acidification in the California current system. *Science* **337**, 220–223. (doi:10.1126/science.1216773)
 16. Somero GN. 2012 The physiology of global change: linking patterns to mechanisms. *Annu. Rev. Mar. Sci.* **4**, 39–61. (doi:10.1146/annurev-marine-120710-100935)
 17. Metzger R, Sartoris FJ, Langenbuch M, Pörtner HO. 2007 Influence of elevated CO₂ concentrations on thermal tolerance of the edible crab *Cancer pagurus*. *J. Therm. Biol.* **32**, 144–151. (doi:10.1016/j.jtherbio.2007.01.010)
 18. Walther K, Sartoris FJ, Bock C, Pörtner HO. 2009 Impact of anthropogenic ocean acidification on thermal tolerance of the spider crab *Hyas araneus*. *Biogeosciences* **6**, 2207–2215. (doi:10.5194/bg-6-2207-2009)
 19. Hochachka PW, Somero GN. 2002 *Biochemical adaptation mechanism and process in physiological evolution*. New York, NY: Oxford University Press.
 20. Sartoris FJ, Bock C, Serendero I, Lannig G, Pörtner HO. 2003 Temperature-dependent changes in energy metabolism, intracellular pH and blood oxygen tension in the Atlantic cod. *J. Fish Biol.* **62**, 1239–1253. (doi:10.1046/j.1095-8649.2003.00099.x)
 21. Johnson CH, Clapper DL, Winkler MM, Lee HC, Epel D. 1983 A volatile inhibitor immobilizes sea-urchin sperm in semen by depressing the intra cellular pH. *Dev. Biol.* **98**, 493–501. (doi:10.1016/0012-1606(83)90378-0)
 22. Fanguie NA, O'Donnell MJ, Sewell MA, Matson PG, MacPherson AC, Hofmann GE. 2010 A laboratory-based, experimental system for the study of ocean acidification effects on marine invertebrate larvae. *Limnol. Oceanogr. Methods* **8**, 441–452. (doi:10.4319/lom.2010.8.441)
 23. Yu PC, Matson PG, Martz TR, Hofmann GE. 2011 The ocean acidification seascape and its relationship to the performance of calcifying marine invertebrates: laboratory experiments on the development of urchin larvae framed by environmentally-relevant pCO₂/pH. *J. Exp. Mar. Biol. Ecol.* **400**, 288–295. (doi:10.1016/j.jembe.2011.02.016)
 24. IPCC. 2007. In *Climate change 2007: the physical science basis* (eds S Solomon, D Qin, M Manning, Z Chen, M Marquis, KB Averyt, M Tignor, HC Miller). Contribution of Working Group I to the Fourth Assessment Report of the Intergovernmental Panel on Climate Change. Cambridge, UK and New York: Cambridge University Press.
 25. Dickson AG, Sabine CL, Christian JR. 2007 *Guide to best practices for ocean CO₂ measurements*, p. 191. Sidney: Canada: PICES – The North Pacific Marine Science Organization.
 26. Robbins LL, Hansen ME, Kleypass JA, Meylan SC. 2010 CO₂calc—A user-friendly seawater carbon calculator for Windows, Max OS X, and iOS (iPhone): U.S. Geological Survey Open-File Report 2010–1280.
 27. Mehrbach C, Culbertson CH, Hawley JE, Pytkowicz RM. 1973 Measurement of the apparent dissociation constants of carbonic-acid in seawater at atmospheric pressure. *Limnol. Oceanogr.* **18**, 897–907. (doi:10.4319/lo.1973.18.6.0897)
 28. Strathmann MF. 1987 *Reproduction and development of marine invertebrates of the northern Pacific coast: data and methods for the study of eggs, embryos, and larvae*. Seattle, WA: University of Washington Press. (doi:10.1093/cercor/12.9.926)
 29. R Development Core Team. 2010 *R: a language and environment for statistical computing*. Vienna, Austria: R Foundation for Statistical Computing.
 30. Marsh AG, Manahan DT. 1999 A method for accurate measurements of the respiration rates of marine invertebrate embryos and larvae. *Mar. Ecol. Progr. Series* **184**, 1–10. (doi:10.1016/0304-3940(95)12056-A)
 31. Randall D, Burggren W, French K. 2001 *Eckert animal physiology*, 5th edn. New York, NY: W.H. Freeman.
 32. Chomczynski P, Sacchi N. 1987 Single-step method of RNA isolation by acid guanidium thiocyanate phenol chloroform extraction. *Anal. Biochem.* **162**, 156–159. (doi:10.1006/abio.1987.9999)
 33. Evans TG, Chan F, Menge BA, Hofmann GE. 2013 Transcriptomic responses to ocean acidification in larval sea urchins from a naturally low pH environment. *Mol. Ecol.* **22**, 1609–1625. (doi:10.1111/mec.12188)
 34. Alter O, Brown PO, Botstein D. 2000 Singular value decomposition for genome-wide expression data processing and modeling. *Proc. Natl Acad. Sci. USA* **97**, 10 101–10 106. (doi:10.1073/pnas.97.18.10101)
 35. Sharov AA, Dudekula DB, Ko MSH. 2005 A web-based tool for principal component and significance analysis of microarray data. *Bioinformatics* **21**, 2548–2549. (doi:10.1093/bioinformatics/bti343)
 36. Huang DW, Sherman BT, Lempicki RA. 2009 Systematic and integrative analysis of large gene lists using DAVID bioinformatics resources. *Nat. Protoc.* **4**, 44–57. (doi:10.1038/nprot.2008.211)
 37. Wilt FH. 1999 Matrix and mineral in the sea urchin larval skeleton. *J. Struct. Biol.* **126**, 216–226. (doi:10.1006/jsbi.1999.4105)
 38. Kurihara H, Shirayama Y. 2004 Effects of increased atmospheric CO₂ on sea urchin early development. *Mar. Ecol. Progr. Ser.* **274**, 161–169. (doi:10.3354/meps274161)
 39. Brennand HS, Soars N, Dworjanyn SA, Davis AR, Byrne M. 2010 Impact of ocean warming and ocean acidification on larval development and calcification in the sea urchin *Tripeustes gratilla*. *PLoS ONE* **5**, e11372. (doi:10.1371/journal.pone.0011372)
 40. Dupont S, Ortega-Martinez O, Thorndyke M. 2010 Impact of near-future ocean acidification on echinoderms. *Ecotoxicology* **19**, 449–462. (doi:10.1007/s10646-010-0463-6)
 41. O'Donnell MJ, Todgham AE, Sewell MA, Hammond LM, Ruggiero K, Fanguie NA, Zippay ML, Hofmann GE. 2010 Ocean acidification alters skeletogenesis and gene expression in larval sea urchins. *Mar. Ecol. Progr. Ser.* **398**, 157–171. (doi:10.3354/meps08346)
 42. Byrne M, Ho M, Wong E, Soars NA, Selvakumaraswamy P, Shepard-Brennand H, Dworjanyn SA, Davis AR. 2011 Unshelled abalone and corrupted urchins: development of marine calcifiers in a changing ocean. *Proc. R. Soc. B* **278**, 2376–2383. (doi:10.1098/Rspb.2010.2404)
 43. Sheridan JA, Bickford D. 2011 Shrinking body size as an ecological response to climate change. *Nat. Climate Change* **1**, 401–406. (doi:10.1038/ndclimate1259)
 44. Allen JD. 2008 Size-specific predation on marine invertebrate larvae. *Biol. Bull.* **214**, 42–49. (doi:10.2307/25066658)
 45. Chan KYK, Grunbaum D, O'Donnell MJ. 2011 Effects of ocean acidification on swimming performance in larval sand dollars and oysters. *Integr. Comp. Biol.* **51**, E22. (doi:10.1016/j.neuropsychologia.2010.08.004)
 46. Strathmann RR. 1971 The feeding behavior of plantotrophic echinoderm larvae mechanisms regulation and rates of suspension feeding. *J. Exp. Mar. Biol. Ecol.* **6**, 109–160. (doi:10.1016/0022-0981(71)90054-2)
 47. Hart MW, Strathmann RR. 1994 Functional consequences of phenotypic plasticity in echinoid larvae. *Biol. Bull.* **186**, 291–299. (doi:10.2307/1542275)
 48. Pennington JT, Strathmann RR. 1990 Consequences of the calcite skeletons of planktonic echinoderm larvae for orientation, swimming, and shape. *Biol. Bull.* **179**, 121–133. (doi:10.2307/1541746)
 49. Strathmann RR, Grunbaum D. 2006 Good eaters, poor swimmers: compromises in larval form. *Integr. Comp. Biol.* **46**, 312–322. (doi:10.1093/icb/ijc031)

50. Stumpp M, Wren J, Melzner F, Thorndyke MC, Dupont ST. 2011 CO₂ induced seawater acidification impacts sea urchin larval development. I. Elevated metabolic rates decrease scope for growth and induce developmental delay. *Comp. Biochem. Physiol. Mol. Integr. Physiol.* **160**, 331–340. (doi:10.1016/j.cbpa.2011.06.022)
51. Michaelidis B, Ouzounis C, Paleras A, Pörtner HO. 2005 Effects of long-term moderate hypercapnia on acid-base balance and growth rate in marine mussels *Mytilus galloprovincialis*. *Mar. Ecol. Progr. Ser.* **293**, 109–118. (doi:10.3354/meps293109)
52. Albright R, Langdon C. 2011 Ocean acidification impacts multiple early life history processes of the Caribbean coral *Porites astreoides*. *Glob. Change Biol.* **17**, 2478–2487. (doi:10.1111/j.1365-2486.2011.02404.x)
53. Fabry VJ, Seibel BA, Feely RA, Orr JC. 2008 Impacts of ocean acidification on marine fauna and ecosystem processes. *ICES J. Mar. Sci.* **65**, 414–432. (doi:10.1093/icesjms/fns048)
54. Todgham AE, Hofmann GE. 2009 Transcriptomic response of sea urchin larvae *Strongylocentrotus purpuratus* to CO₂-driven seawater acidification. *J. Exp. Biol.* **212**, 2579–2594. (doi:10.1242/jeb.032540)
55. Hammond LM, Hofmann GE. 2012 Early developmental gene regulation in *Strongylocentrotus purpuratus* embryos in response to elevated CO₂ seawater conditions. *J. Exp. Biol.* **215**, 2445–2454. (doi:10.1242/jeb.058008)
56. Place SP, Smith BW. 2012 Effects of seawater acidification on cell cycle control mechanisms in *Strongylocentrotus purpuratus* embryos. *PLoS ONE* **7**, e34068. (doi:10.1371/journal.pone.0034068)
57. Byrne M, Ho M, Selvakumaraswamy P, Nguyen HD, Dworjanyn SA, Davis AR. 2009 Temperature, but not pH, compromises sea urchin fertilization and early development under near-future climate change scenarios. *Proc. R. Soc. B* **276**, 1883–1888. (doi:10.1098/Rspb.2008.1935)
58. Nguyen HD, Doo SS, Soars NA, Byrne M. 2012 Noncalcifying larvae in a changing ocean: warming, not acidification/hypercapnia, is the dominant stressor on development of the sea star *Meridiastra calcar*. *Glob. Change Biol.* **18**, 2466–2476. (doi:10.1111/j.1365-2486.2012.02714.x)
59. Miner BG. 2005 Evolution of feeding structure plasticity in marine invertebrate larvae: a possible trade-off between arm length and stomach size. *J. Exp. Mar. Biol. Ecol.* **315**, 117–125. (doi:10.1016/j.jembe.2004.09.011)
60. Anderson D, Hedgecock D. 2010 Inbreeding depression and growth heterosis in larvae of the purple sea urchin *Strongylocentrotus purpuratus* (Stimpson). *J. Exp. Mar. Biol. Ecol.* **384**, 68–75. (doi:10.1016/j.jembe.2009.12.005)
61. Adams DK, Sewell MA, Angerer RC, Angerer LM. 2011 Rapid adaptation to food availability by a dopamine-mediated morphogenetic response. *Nat. Commun.* **2**, 592. (doi:10.1038/ncomms1603)
62. Guss KA, Ettensohn CA. 1997 Skeletal morphogenesis in the sea urchin embryo: regulation of primary mesenchyme gene expression and skeletal rod growth by ectoderm-derived cues. *Development* **124**, 1899–1908. (doi:10.1152/jn.00339.2011)
63. Katada S, Imhof A, Sassone-Corsi P. 2012 Connecting threads: epigenetics and metabolism. *Cell* **148**, 24–28. (doi:10.1016/j.cell.2012.01.001)
64. Su C, Gao G, Schneider S, Helt C, Weiss C, O'Reilly MA, Bohman D, Zhao JY. 2004 DNA damage induces downregulation of histone gene expression through the G₁ checkpoint pathway. *Embo J.* **23**, 1133–1143. (doi:10.1038/sj.emboj.7600120)
65. Cohen I, Poreba E, Kamieniarz K, Schneider R. 2011 Histone modifiers in cancer: friends or foes? *Genes Cancer* **2**, 631–647. (doi:10.1017/S0140525X00057678)
66. Kouzarides T. 2007 Chromatin modifications and their function. *Cell* **128**, 693–705. (doi:10.1016/j.cell.2007.02.005)
67. Kamemura K, Ogawa M, Ohkubo S, Ohtsuka Y, Shitara Y, Komiya T, Maeda S, Ito A, Yoshida M. 2012 Depression of mitochondrial metabolism by downregulation of cytoplasmic deacetylase, HDAC6. *Febs Lett.* **586**, 1379–1383. (doi:10.1016/j.febslet.2012.03.060)
68. Clapier CR, Cairns BR. 2009 The biology of chromatin remodeling complexes. *Annu. Rev. Biochem.* **78**, 273–304. (doi:10.1146/annurev.biochem.77.062706.153223)
69. Guppy M, Withers P. 1999 Metabolic depression in animals: physiological perspectives and biochemical generalizations. *Biol. Rev. Camb. Phil. Soc.* **74**, 1–40. (doi:10.1017/s0006323198005258)
70. Morris RL *et al.* 2006 Analysis of cytoskeletal and motility proteins in the sea urchin genome assembly. *Dev. Biol.* **300**, 219–237. (doi:10.1016/j.ydbio.2006.08.052)
71. Lockwood BL, Sanders JG, Somero GN. 2010 Transcriptomic responses to heat stress in invasive and native blue mussels (genus *Mytilus*): molecular correlates of invasive success. *J. Exp. Biol.* **213**, 3548–3558. (doi:10.1242/jeb.046094)
72. Tomanek L, Zuzow MJ. 2010 The proteomic response of the mussel congeners *Mytilus galloprovincialis* and *M. trossulus* to acute heat stress: implications for thermal tolerance limits and metabolic costs of thermal stress. *J. Exp. Biol.* **213**, 3559–3574. (doi:10.1242/jeb.041228)
73. Hofmann GE, Barry JP, Edmunds PJ, Gates RD, Hutchins DA, Klinger T, Sewell MA. 2010 The effect of ocean acidification on calcifying organisms in marine ecosystems: an organism-to-ecosystem perspective. *Annu. Rev. Ecol. Syst.* **41**, 127–147. (doi:10.1146/annurev.ecolsys.110308.120227)